AIP Applied Physics Letters

Refractive index sensor based on hybrid coupler with short-range surface plasmon polariton and dielectric waveguide

Boyu Fan, Fang Liu, Yunxiang Li, Yidong Huang, Yoshikatsu Miura, and Dai Ohnishi

Citation: Applied Physics Letters **100**, 111108 (2012); doi: 10.1063/1.3693408
View online: http://dx.doi.org/10.1063/1.3693408
View Table of Contents: http://scitation.aip.org/content/aip/journal/apl/100/11?ver=pdfcov
Published by the AIP Publishing

Refractive index sensor based on hybrid coupler with short-range surface plasmon polariton and dielectric waveguide

Boyu Fan,[1] Fang Liu,[1,a)] Yunxiang Li,[1] Yidong Huang,[1] Yoshikatsu Miura,[2] and Dai Ohnishi[2]
[1]*State Key Lab of Integrated Optoelectronics, Tsinghua National Laboratory for Information Science and Technology, Department of Electronic Engineering, Tsinghua University, Beijing 100084, China*
[2]*Photonics R&D Center, ROHM Co., Ltd., Kyoto 615-8585, Japan*

(Received 26 October 2011; accepted 23 February 2012; published online 13 March 2012)

An integrated sensor based on a vertical hybrid coupler composed of a short-range surface plasmon polariton (SRSPP) waveguide and a SiN_x dielectric waveguide has been realized. The output power of the sensor is observed to change drastically with the refractive index of the detection liquid, and the sensing region can be adjusted by varying the width of the SiN_x waveguide. The resolution is estimated to be as high as 7.3×10^{-6} refractive index units. This sensor is expected to have significantly high effective sensitivity for detecting a hundred-nanometer-thick layer owing to the highly bounded field of the SRSPP mode. © *2012 American Institute of Physics*. [http://dx.doi.org/10.1063/1.3693408]

A surface plasmon polariton (SPP) is a transverse-magnetic surface electromagnetic excitation that propagates along an interface between a metal and a dielectric medium.[1] Owing to its high sensitivity to the refractive index of the dielectrics on a metal surface, the application of SPP in biological and chemical sensing has received extensive attention.[2–10] However, the sensitivity of the traditional SPP sensor declines significantly when the thickness of the detection layer is only in the range of tens or hundreds of nanometers. This is because the sensing region is significantly thinner than the field penetration depth of the general SPP mode, and the SPP cannot effectively register the refractive index change in such a thin detection layer.

The short-range SPP (SRSPP) mode is a type of SPP mode guided by a thin metal film with its field highly bounded to the surface of the metal to a depth of hundreds of nanometers,[2] which is promising for ultrathin layer detection.[2] Recently, our group demonstrated theoretically and experimentally that SRSPP mode can be excited efficiently based on a vertical hybrid coupler composed of a thin metal film and a dielectric waveguide.[11,12] In addition, it has been demonstrated theoretically that the coupling between the SPP mode and the dielectric waveguide mode is very sensitive to the refractive index of dielectrics on the metal surface, which is promising for the realization of an integrated SPP sensor with high sensitivity. In this work, a compact integratable sensor based on the vertical SRSPP-SiN_x hybrid coupler, with a sensing region of only 110 μm length, has been fabricated and studied. The output power varying drastically with the refractive index of the detection layer n_{det} has been observed with the refractive index variations as small as 7.3×10^{-6} RIU. This sensor is expected to have a significantly high sensitivity when applied to ultra-thin layer detection (for a thickness of approximately 1/10th of the wavelength in vacuum[13]) of small bio- or chemical molecules, owing to the highly bounded field of the SRSPP mode. Furthermore, it is observed that the sensing range can be adjusted by varying the width of the dielectric waveguide, making the design and application of the sensor more flexible.

Figure 1 shows the schematic structure of the integrated sensor, which is based on a hybrid coupler composed of a SRSPP waveguide (Au strip with thickness T_m, width W_m, and dielectric constant ε_m) and a dielectric waveguide (DW) (SiN_x strip with thickness T_d, width W_d, and refractive index n_d). The distance between the two waveguides is D. The dielectrics surrounding the two waveguides are SiO_2 with refractive index n_s. Above the SRSPP waveguide, there is the sensing window with length L along the z-direction, in which the refractive index of the detection layer (n_{det}) is variable. The sectional view of the hybrid coupler sensor in the x–y

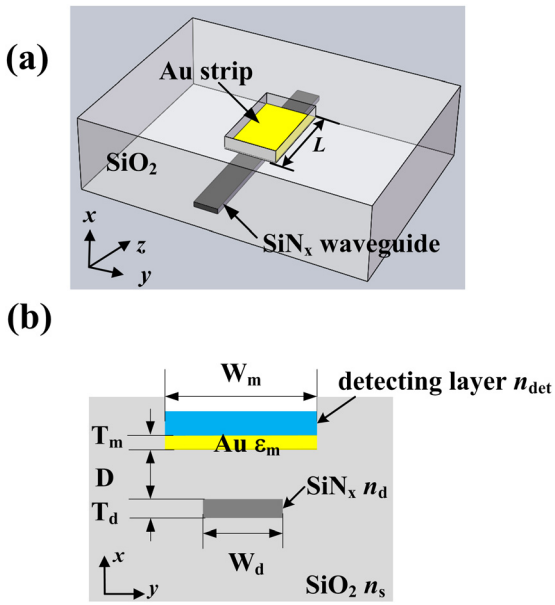

FIG. 1. (Color online) (a) Schematic structure of the integrated sensor based on the SRSPP-SiN_x vertical coupler with Au strip (yellow) and SiN_x strip (gray) embedded in SiO_2. (b) Sectional view of the sensor in the x–y plane.

a)Author to whom correspondence should be addressed. Electronic mail: liu_fang@tsinghua.edu.cn.

plane and the detailed structure parameters are presented in Fig. 1(b).

To calculate the sensing characteristics, namely the change in the output power with the refractive index n_{det}, this integrated sensor is divided into three parts along the z-direction (the input and output region, consisting only of the SiN_x waveguide, and the sensing region, composed of hybrid waveguides structure). The detailed simulation method is similar to that described in Ref. 11, the difference being that the eigenmodes in the x–y plane should be calculated with the finite element method (FEM). According to Ref. 11, the TM mode in the sensing region can be expressed with the two eigenmodes as follows:

$$H(x,y,z) = \sum_{m=A,B} \alpha_m e^{-\beta_{mi} z} H_m(x,y) e^{-i\beta_{mr} z}, \quad (1)$$

where H_A and H_B are the complex magnetic fields of modes A and B ($z=0$), and $\alpha_m = \frac{1}{2}\int (E_d \times H_m) \cdot \hat{z} dx$ and $\beta_m = \beta_{mr} - i \times \beta_{mi} (m = A, B)$ are the coupling coefficient and the complex propagation constant of the eigenmodes in the sensing region, respectively.

After a propagation length L, the TM polarized output power of the DW, P_{out}, can be expressed as

$$P_{out} = -20\lg\left(\left|\frac{1}{2}\int (E_d \times H(x,y,z=L)) \cdot \hat{z} dA\right|\right) = -20\lg\left(\left|\sum_{m=A,B} \alpha_m^2 e^{-\beta_{mi} L} e^{-i\beta_{mr} L}\right|\right). \quad (2)$$

Since the coupling between the SRSPP and the DW mode is sensitive to n_{det}, the output power of the DW, P_{out}, is also extremely sensitive to n_{det}. Figure 2 shows that P_{out} varies drastically with n_{det} for different widths of the DW by setting $L = 110\,\mu m$. The dips of the curves in Fig. 2 and the variation in P_{out} over the corresponding change in n_{det} are defined as the sensing center and the sensitivity,[2] respectively. Taking $W_d = 3\,\mu m$ as an example, with a sensing center of 1.445, the average sensitivity when n_{det} varies from 1.445 to 1.45 is approximately 8880 dB/RIU. For the assumption that the resolution of the power meter is 0.01 dB,[2] the minimum detectable refractive index change can be as small as 1.1×10^{-6} RIU. Compared with a traditional integrated SPP sensor,[7–9] the SRSPP-dielectric coupling sensor has the potential for sensing ultrathin films with a higher sensitivity, owing to the highly concentrated mode field of the SRSPP.[13] Furthermore, by comparing the three curves in Fig. 2, it can be seen that the sensing center increases with the width of the DW, i.e., W_d, which provides a method that can be used to design the sensor in a more flexible manner. Here, the shift of the curve is because both the sensing center and the best coupling point (as well as the sensing center) between the SRSPP mode and the DW mode change when adjusting W_d.

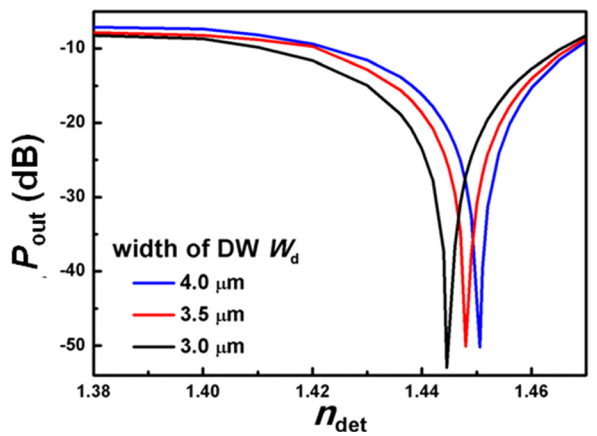

FIG. 2. (Color online) Output power P_{out} as a function of n_{det} labeled with different widths of the DW, i.e., W_d. Here, $\lambda = 1.55\,\mu m$, $n_d = 2$, $n_s = 1.444$, $\varepsilon_m = -132 + i \times 12.65$,[14] $T_d = 175\,nm$, $T_m = 17\,nm$, $W_m = 8\,\mu m$, and $D = 1.5\,\mu m$.

To fabricate this sensor, a Si wafer with a 15 μm-thick SiO_2 layer on the surface is selected as the substrate. On the substrate, a layer of SiN_x with a thickness of $T_d = 175\,nm$ is deposited by plasma-enhanced chemical-vapor deposition (PECVD). After standard UV lithography, reaction ion etching (RIE), and photoresist removal, SiN_x strips with different widths W_d (2.5, 3, 3.5, 4, 4.5, and 5 μm) are obtained. Covering the SiN_x strips with a $D = 1.5\,\mu m$-thick SiO_2 layer by PECVD, the fabrication of the SiN_x waveguide is completed. Then, a groove structure with length $L = 110\,\mu m$ is formed on this 1.5 μm-thick SiO_2 layer by cover-lithography and a wet etching process using buffered hydrofluoric acid (BHF). The depth of the groove (namely, the distance D between the SiN_x strip and the Au strip) is controlled by the concentration of BHF and the etching time. Further, after sputtering an Au film with a thickness of $T_m = 17\,nm$ by magnetic sputtering and then lifting off the photoresist and Au film outside the groove structure, the fabrication of the sensor based on the hybrid coupler is completed. Figure 3 shows microscope images of the integrated sensor based on the SRSPP-SiN_x coupler, where the yellow strip (Au) is the SRSPP waveguide and the light gray strip is the SiN_x waveguide.

Here, the chip is cut into 2.5-mm-long pieces for easier measurement, though the length of the vertical hybrid coupler L (sensing length) is only 110 μm. The measurement system consisted of a laser emitting at a wavelength of 1.55 μm, a polarization controller, an input and output tapered-lens fibers, a precise fiber alignment system controlled by computer, and a power meter. In the fiber-to-waveguide butt-coupling measurement, the detection liquid is dropped onto the sensor chip, and subsequently, the output powers of the TE and TM modes are obtained by switching the input polarized modes. The detection liquids are from Cargille Labs with certified refractive indices of 1.4, 1.41, 1.42, 1.43, 1.44, 1.45, 1.46, and 1.47, respectively. To obtain detection liquids with a refractive index between 1.4 and 1.47, the certified refractive index liquids are mixed in the proper proportion, and the refractive index is checked by an

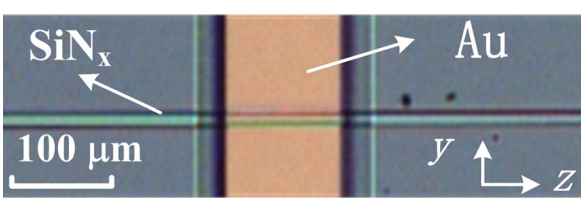

FIG. 3. (Color online) Optical microscopy images of the integrated sensor based on the SRSPP-SiN_x coupler.

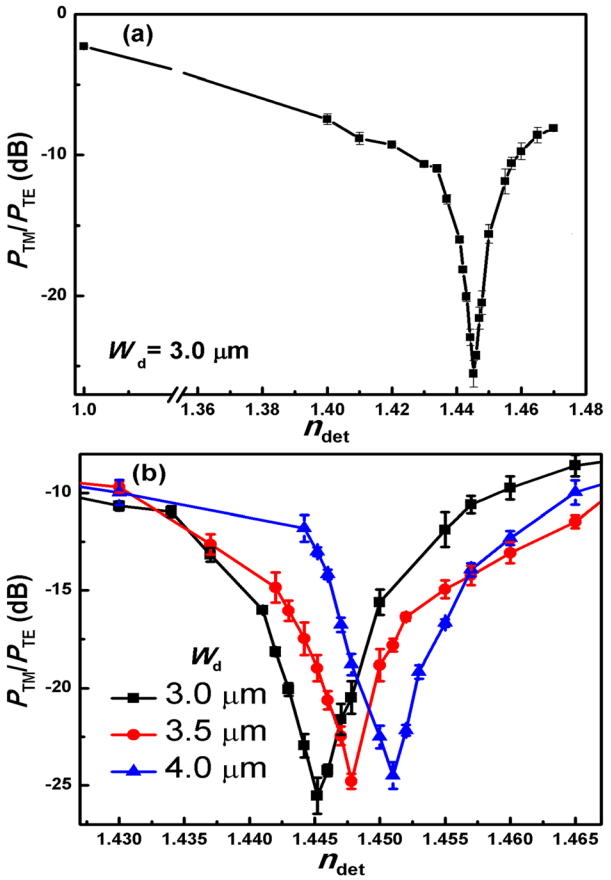

FIG. 4. (Color online) (a) The measured output P_{TM}/P_{TE} ratio (black triangles with error-bar) versus the refractive index of the detection layer n_{det} when the width of the SiN_x waveguide is $W_d = 3.0\,\mu m$. Here, all the inputs were applied to the SiN_x strip. (b) The range of sensing centers of the measured results labeled with different widths (W_d) of the DW.

Abbe refractometer. After obtaining the output power of the sensor under a certain refractive index liquid, the sensor chip is cleaned by phenoxin, ethanol, and deionized water to remove the detection liquid. The measurement is then repeated by varying the refractive index of the detection liquid.

Since there is no coupling between the TE mode and the SRSPP mode,[11,12] it was observed that the TE-polarized output power changed negligibly with n_{det} and that the loss was as low as 0.2 dB for the sensor with a sensing length of 110 μm; this is consistent with the theoretical prediction. Therefore, the output power of the TM mode (P_{TM}) could be normalized with that of the TE mode (P_{TE}) to eliminate the influence of the alignment between the input/output fibers and the SiN_x waveguide.

Figure 4 shows the measurement results of the output power P_{TM}/P_{TE} (dB) from the SiN_x waveguide versus the refractive index of the detection liquid n_{det}, which is normalized by the output power ratio P_{TM0}/P_{TE0} without the detection liquid ($n_{det} = 1$). Each curve is derived by measuring three sensors with the same structure parameters, and the small error bars indicate that the sensors have good consistency in sensing performance. For the sensor with $W_d = 3\,\mu m$, it is shown in Fig. 4(a) that the ratio P_{TM}/P_{TE} changes drastically with n_{det} values in the vicinity of 1.445, which corresponds to the different energy coupling efficiencies between the SRSPP mode and the TM mode of the SiN_x waveguide under different values of n_{det}. It is estimated that the average sensitivity for n_{det} in the range of 1.445–1.455 is approximately 1365 dB/RIU. Assuming the resolution of the power meter to be 0.01 dB,[2] the minimum detectable refractive index change can be as small as 7.3×10^{-6} RIU.

The simulation result shown in Fig. 2 indicates that the sensing center could be adjusted by varying the width of the SiN_x waveguide. To verify this simulation result, sensors with different W_d are fabricated, and the subsequent measurement result is shown in Fig. 4(b). For the sensors with $W_d = 3.5\,\mu m$ and 4.0 μm, a similar sensing curve of P_{TM}/P_{TE} vs. n_{det} has also been observed, and their sensing centers increased to 1.448 and 1.451, respectively. A 0.5 μm increase in W_d is shown to correspond to a 3.0×10^{-3} increase in the sensing center, which is well fitted by the simulated results shown in Fig. 2.

In conclusion, a highly integrated sensor based on a vertical SRSPP-dielectric hybrid coupler has been realized. It is observed that the TM-polarized output power varies drastically with the refractive index of the detection liquid, and the minimum detectable refractive index change is as small as 7.3×10^{-6}. Meanwhile, by changing the width of the SiN_x waveguide W_d, the sensing center can be adjusted easily. Considering the highly bounded field of the SRSPP mode on the metal surface, this sensor would have significantly high effective sensitivity for ultra-thin film or small molecule detection.[13]

This work is supported by the National Basic Research Programs of China (973 Program) under Contract Nos. 2011CB301803, 2010CB327405, and 2011CBA00608, and by the National Natural Science Foundation of China (NSFC-61036011, 61107050, and 61036010). The authors thank Professor Jiangde Peng, Professor Wei Zhang, Dr. Xue Feng, and Kaiyu Cui, as well as Mr. H. Takatsu and A. Kamisawa of the ROHM Corporation, for their helpful comments.

[1]J. J. Bruke and G. I. Stegeman, Phys. Rev. B **33**, 5186 (1986).
[2]J. Homola, S. S. Yee, and G. Gauglitz, Sens. Actuators B **54**, 3 (1999).
[3]J. Homola, Anal. Bioanal. Chem. **377**, 528 (2003).
[4]X. D. Hoa, A. G. Kirk, and M. Tabrizian, Biosens. Bioelectron. **23**, 151 (2007).
[5]M. Vala, J. Dostálek, and J. Homola, Proc. SPIE **6585**, 658522 (2007).
[6]J. Guo, P. D. Keathley, and J. T. Hastings, Opt. Lett. **33**, 512 (2008).
[7]E. K. Akowuah, T. Gorman, and S. Haxha, Opt. Express **17**, 23511 (2009).
[8]Y. H. Joo, S. H. Song, and R. Magnusson, Appl. Phys. Lett. **97**, 201105 (2010).
[9]M.-S. Kwon, Opt. Lett. **35**, 3835 (2010).
[10]M. N. Weiss, R. Srivastava, H. Groger, P. Lo, and S. F.Luo, Sens. Actuators A **51**, 211 (1996).
[11]R. Wan, F. Liu, X. Tang, Y. Huang, and J. Peng, Appl. Phys. Lett. **94**, 141104 (2009).
[12]R. Wan, F. Liu, Y. Huang, B. Fan, Y. Miura, D. Ohnishi, Y. Li, H. Li, and Y. Xia, Appl. Phys. Lett. **97**, 141105 (2010).
[13]R. Wan, F. Liu, and Y. Huang, Opt. Lett. **35**, 244 (2010).
[14]E. D. Palik, *Handbook of Optical Constants of Solids* (Academic, Orlando, FL, 1985).